Impedance and initial magnetic permeability of the Heusler compounds Pd_2MnSn and Pd_2MnSb near the Curie temperature

G. L. Ferreira-Fraga,* L. A. Borba, and P. Pureur
Instituto de Física, Universidade Federal do Rio Grande do Sul (UFRGS), Porto Alegre 91501-970, RS, Brazil
(Received 18 January 2006; revised manuscript received 5 June 2006; published 31 August 2006)

In this paper we report measurements of the complex impedance of the Heusler compounds Pd_2MnSn and Pd_2MnSb near the Curie temperature. From the experimental data, the complex initial magnetic permeability is obtained as a function of temperature and frequency. Both the real μ' and the imaginary μ'' components of the permeability show a sharp maximum at a characteristic temperature T_{peak} which is located just below T_c. This property is known as the Hopkinson effect. In low frequencies this effect is more pronounced in Pd_2MnSn. We attribute the high values of μ' obtained in this compound to a high density of domain walls generated by antiphase boundaries (APBs). We show that μ' behaves as a critical power law of the reduced temperature $1-T/T_c$ below T_{peak} in both compounds. Above T_{peak}, μ' may also be described by a power law of $1-T/T_c$ with an unusually large exponent. We argue that a crossover between two different domain-wall fluctuation regimes occurs at this temperature. A Cole-Cole analysis allows the determination of the relaxation time distribution at several fixed temperatures in the ferromagnetic region of Pd_2MnSn. These results were fitted to a modified Debye formula. The obtained fit parameters indicate that the dynamical properties of the permeability in this compound are governed by a broad and temperature-independent distribution of relaxation times. This behavior is characteristic of a system where magnetic domains are distributed within a large range of sizes that do not change significantly when the temperature approaches T_c.

DOI: 10.1103/PhysRevB.74.064427 PACS number(s): 75.30.Kz, 72.15.Eb, 75.47.Np

I. INTRODUCTION

An ac current flowing along the axis of a cylindric conductor generates an alternated circumferential magnetic field. When the conductor is ferromagnetic, this field magnetizes transversally the material. At high frequencies the current tends to concentrate near the surface of the conductor because of the skin effect. The impedance Z is the linear response function that relates the complex representation of the current distribution inside the conducting material to the measured voltage between two points at different electrical potential, $V(\omega)=ZI(\omega)$.

The impedance depends on the shape of the conductor, frequency of the alternating current, and also on the magnetic permeability μ of the material. Impedance measurements are quite useful to study soft ferromagnets. Since the permeability in this case is strongly dependent on externally applied fields, giant magnetoimpedance effects may be produced.[1] The temperature-driven magnetic phase transition also generates intrinsic impedance effects below T_c that may be quite strong.[2] Impedance experiments have also been used to study magnetic transition in nanocrystalline soft magnetic alloys [3] and as an auxiliary experimental technique to detect weak-order magnetic or structural transitions.[4] For certain sample's geometries, the complex magnetic permeability may be directly estimated from impedance results and, in the cases where the permeability depends on the frequency of the driving current, these measurements may be used as an useful tool to study the dynamical properties of ferromagnetic materials.[5]

Much less studied is the temperature and field dependence of the impedance near magnetic transitions.[2] One important property that may be clearly observed in these experiments is the Hopkinson effect.[6] This property accounts for the maximum shown by the initial magnetic permeability of ferromagnetic materials just below the Curie temperature T_c. This thermomagnetic effect has been observed in many hard ferromagnetic materials with fine grain structure,[7] soft magnetic ferrites,[8–10] and ferromagnetic amorphous alloys.[11] The mechanism responsible for the Hopkinson effect is a subject of controversy. Domain-wall displacements and rotation of the magnetization are frequently evoked to explain its origin.[8,12,13] It has also been argued[14] that the magnetocrystalline anisotropy plays an important role in some cases. Another line of interpretation relates the Hopkinson effect to a phase transition involving the detailed domain structure of anisotropic ferromagnetic materials.[15]

The Hopkinson effect has been mostly observed in magnetization and ac susceptibility measurements. However, one expects that new insights about its origin may be provided by transport measurements in a zero-applied field. In this case, the demagnetizing effect does not play a role due to the circumferential exciting magnetic field.

In this work we study the impedance of the intermetallic Heusler compounds Pd_2MnSn and Pd_2MnSb.[16] These ternary compounds crystallize with the $L2_1$ cubic structure.[17] Below 178 K and 240 K, respectively, they undergo a magnetic transition to a ferromagnetic state. The magnetism is due to Mn atoms having a magnetic moment of approximately $4\mu_B$. Since the Mn atoms are widely separated by nonmagnetic atoms, the magnetic order in these compounds is mediated by the indirect Ruderman-Kittel-Kasuya-Yoshida (RKKY) coupling via conduction electrons.

It is well known that the magnetic properties of Pd_2MnSn show an anomalous behavior under cold working.[18] Particularly, the magnetization is drastically reduced without significantly changing the Curie temperature when samples of this compound are crushed into powder.[18] The magnetization

may be partially retrieved by subsequent annealing. This behavior is uncommon among the Heusler compounds. Most of the ferromagnetic Heusler systems, including Pd_2MnSb, do not show appreciable magnetization changes under cold working. The reduction of the magnetization in Pd_2MnSn is explained by the dislocation theory.[19] When placed close to planar dislocations formed by plastic deformations, the Mn spins couple antiferromagnetically, producing structures of anti-parallel magnetic domains that decrease the overall magnetization. Families of narrow domains separated by these anti-phase boundaries (APBs) are distributed heterogeneously in the crystal lattice of plastic deformed Pd_2MnSn, according to transmission electron microscopy studies.[20]

Impedance measurements on polycrystalline samples of Pd_2MnSn and Pd_2MnSb were reported on a previous paper[2] as a function of temperature and external magnetic field for frequencies of the alternating current varying from 25 Hz to 5 kHz. In the present work, we extend the frequency range up to 100 kHz. Improvements on the experimental apparatus allowed a more precise discrimination of the real R and imaginary X components of the complex impedance, $Z=R+iX$. A computational analysis was used to obtain the initial magnetic permeability as a function of frequency and temperature from the experimental impedance data.

The aim of this work is twofold. First is to show that the impedance measurements can be an important tool to study magnetic transitions and the dynamical properties of soft magnetic materials. Second is to point out that the anomalous magnetic behavior of the compound Pd_2MnSn, that is associated to the APB's, can be related to the high initial magnetic permeability observed at low frequencies in this compound.

II. IMPEDANCE AND INITIAL MAGNETIC PERMEABILITY

Under certain symmetry conditions, the relation between the complex impedance and the effective initial magnetic permeability, $\mu=\mu'+i\mu''$, can be easily obtained by solving the Maxwell equations for the magnetic and electrical fields existing inside the conductor.[21] In the quasistatic regime, for a cylindrical conductor of diameter $2a$ and electrical resistance R_{dc}, the complex impedance is given by

$$Z = R_{dc} ka \frac{J_0(ka)}{2J_1(ka)}, \tag{1}$$

where the J_n are Bessel functions of the first kind and $k=(1+i)/\delta$. The skin depth parameter δ describes the radial decay of the current density inside the conductor and is expressed as

$$\delta = \left(\frac{\rho}{\pi f \mu \mu_0} \right)^{1/2}, \tag{2}$$

where ρ is the electrical resistivity, f is the frequency of the alternating current, and μ_0 is the vacuum permeability. Assuming a simple picture without considering magnetic domains, the dependence of the impedance with temperature, frequency, and external magnetic field is governed mainly by the effective and complex magnetic permeability $\mu(T,H,f)$. Thus, the challenge of describing the impedance and magnetoimpedance responses of a magnetic material is basically equivalent to the problem of understanding the behavior of its permeability.

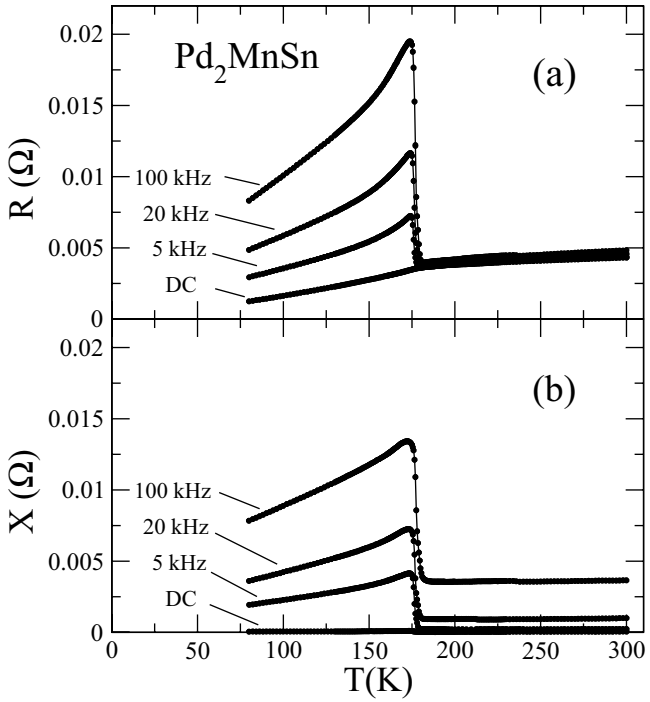

FIG. 1. (a) In-phase resistive and (b) out-of-phase reactive components of the impedance versus temperature for Pd_2MnSn at several frequencies. The amplitude of the *ac* current is 10 mA. The solid lines are guides for the eyes.

III. EXPERIMENTS

The compounds studied in this work where obtained by melting together appropriate amounts of the high purity starting metals in an induction furnace under argon atmosphere. Samples in the form of a parallelepiped, with dimensions of about $1\times1\times14$ mm^3 were cut by spark erosion from the obtained ingot and annealed at 750 °C during three days. Details of the samples' preparation may be found in Ref. 22. Measurements were made with a homemade apparatus based on a four-contacts *ac* technique that employs a dual phase lock-in amplifier as the signal detector. Low ohmic electrical contacts were spark welded on the samples, so that the voltage leads were placed nearly 10 mm apart. The current was supplied by a RF generator operating on a sinusoidal mode with frequency varying between 25 Hz and 100 kHz and fixed RMS amplitude of 10 mA. A 50 ohm resistor was put in a series with the sample in order to achieve the best matching with the impedance of the coaxial cables. The resistance of the samples was very small compared to the total circuit resistance, so that the probe current remained constant during the experiment. In order to improve the accuracy and reliability of the technique to discriminate the in-phase (resistive) and the out-of-phase (reactive) signals, a voltage

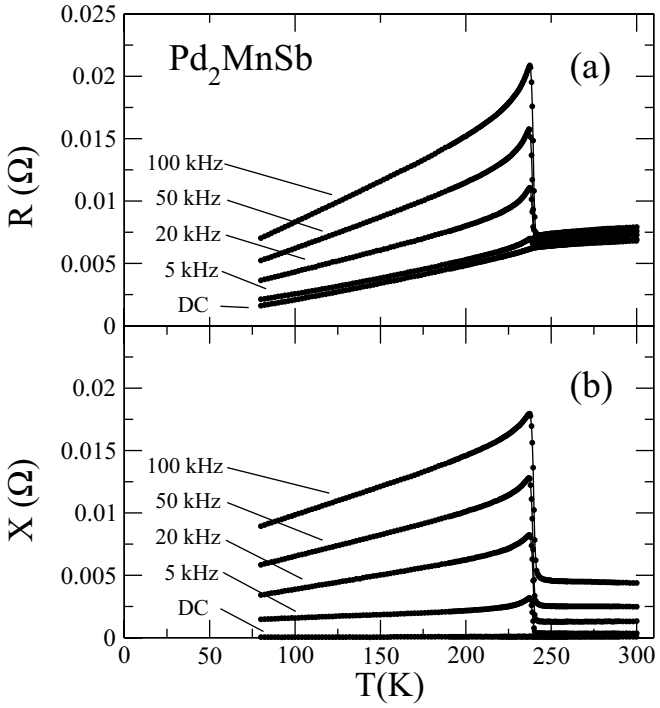

FIG. 2. (a) Resistive and (b) reactive components of the impedance versus temperature for Pd_2MnSb at several frequencies. The amplitude of the *ac* current is 10 mA. The solid lines are guides for the eyes.

drop across a noninductive resistor was used as the reference signal for the lock-in amplifier. Temperatures were measured with a carbon-glass resistor and stabilized within 0.01 K during data recording.

IV. RESULTS

A. Impedance

Measurements of the resistive (R) and reactive (X) components of the impedance versus temperature in several frequencies are shown in Figs. 1 and 2 for Pd_2MnSn and Pd_2MnSb, respectively. As shown in these curves, both samples present a qualitatively similar behavior. A remarkable feature is the steep increase followed by a sharp maximum in both $R(T)$ and $X(T)$ that occurs when the temperature is decreased closely below T_c. This is a manifestation of the Hopkinson effect. The steplike variation of the impedance components near T_c, as well as their magnitudes in the ordered phase, are enhanced when the frequency of the driving current is increased. The resistance and the reactance decrease steadily when the temperature is further decreased, as expected in a ferromagnetic conductor.

The overall behavior shown in Figs. 1 and 2 can be understood with the basis on Eqs. (1) and (2). Clearly, the effective initial permeability should diverge critically at the Curie temperature as the susceptibility when T_c is approached from above. In the ferromagnetic phase μ becomes much larger than the unitary value typical of the paramagnetic state. On the other hand, the frequency variation of R and X is due to the skin-depth effect as given by Eq. (2). An inspection of the curves in Figs. 1 and 2 shows that at $f=100$ kHz both samples present similar magnitudes for the resistive component ratio $(R-R_{dc})/R_{dc}$. Nevertheless, at $f=5$ kHz this ratio is one order of magnitude larger for Pd_2MnSn than for Pd_2MnSb.

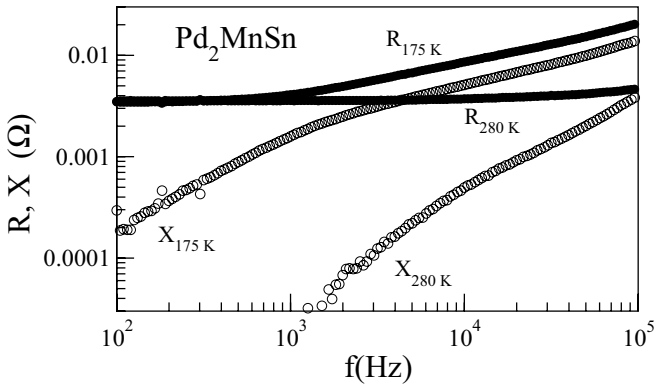

FIG. 3. Frequency dependencies of resistance (•) and reactance (◦) for Pd_2MnSn at 273 K (ferromagnetic phase) and 280 K (paramagnetic phase). Reactances are corrected for external contributions. The amplitude of the alternating current is 10 mA.

Measurements of the complex impedance versus frequency were performed for both samples at several temperatures. Representative examples of these curves are shown in Fig. 3 for Pd_2MnSn at temperatures of 175 K (ferromagnetic phase) and 280 K (paramagnetic phase). In the paramagnetic phase, the resistance $R_{280\ K}$ is nearly constant in the whole frequency range, whereas the reactance $X_{280\ K}$ is very small at low frequencies and becomes an approximately linear function of f above 10 kHz. In the ferromagnetic phase, the impedance shows a quite distinct frequency-dependent behavior. The resistance is constant up to $f=1$ KHz, then increases continuously above this value. The reactance is much higher than in the paramagnetic phase and increases steadily with the frequency.

In the high-frequency range, the reactance behaves similarly to the resistance. The isothermal curves in Fig. 3 may be understood with the basis on the classical skin depth effect. Assuming that $\mu=250$ at $T=173$ K (see Fig. 4) and considering $f=100$ kHz in Eq. (2), we estimate $\delta=0.06$ mm. In this case, the skin depth is smaller than the sample thickness and the current circulates in a thin layer near the sample's surface. The effective cross section for electron transport is reduced, originating the augmented value for the real component of the impedance. On the other hand, $\mu=1$ at $T=280$ K, and from Eq. (2) we estimate $\delta=1$ mm, i.e., the skin depth is of the order of the sample's thickness and the current is uniformly distributed inside the conductor.

B. Magnetic permeability

The initial magnetic permeabilities of Pd_2MnSn and Pd_2MnSb were determined from a computational analysis of the experimental data in Figs. 1 and 2. The samples have the form of a tetragonal parallelepiped. Due to the lack of a

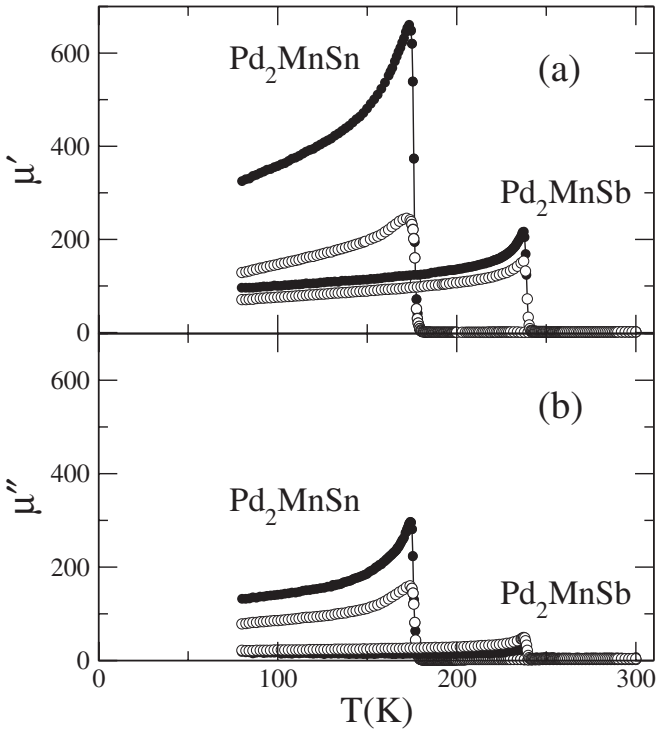

FIG. 4. Temperature dependence of the (a) real and (b) imaginary components of the complex permeability for Pd_2MnSn and Pd_2MnSb at frequencies of 5 kHz (full circles) and 100 kHz (open circles). The solid lines are guides for the eyes.

general analytical expression for calculating the impedance of a sample with this geometry, Eq. (1) was assumed to describe the data. This approximation becomes reasonable when one considers the cylinder diameter in Eq. (1) as equal to the square side of the parallelepiped cross section. Using this procedure, the errors in the normalized resistance, R/R_{DC}, and in the normalized inductive reactance, X/R_{DC}, are smaller than 4% and 10%, respectively. These errors were estimated by numerically calculating the impedance components with the software *Finite Elements Method Magnetics* (FEMM).[23]

The procedure employed to determine the temperature dependence of the magnetic permeability was divided on two steps. First, the external contribution to the impedance in Eq. (1) was estimated as follows. Using the FEMM software, the impedance of a parallelepiped with $\mu=1$ and having the same dimensions of our samples was simulated. Then, the reactive component of this simulated impedance was subtracted from the experimental result at 300 K. In this temperature the samples are in the paramagnetic phase, far above T_c. The obtained difference was attributed to the external reactance, that can attain 3.5 mΩ for $f=100$ kHz. This extrinsic contribution was then subtracted from the impedance data in the whole temperature range. We assume that the external impedance remains constant when the sample is cooled below room temperature. The next step was the determination of the complex magnetic permeability, $\mu=\mu'+i\mu''$. This was achieved by simultaneously solving the equations $R=\mathrm{Re}[Z(T,\mu)]/R_{dc}$ and $X^*=\mathrm{Im}[Z(T,\mu)]/R_{dc}$, where X^* is the reactance corrected as described above and Z is given by Eq. (1).

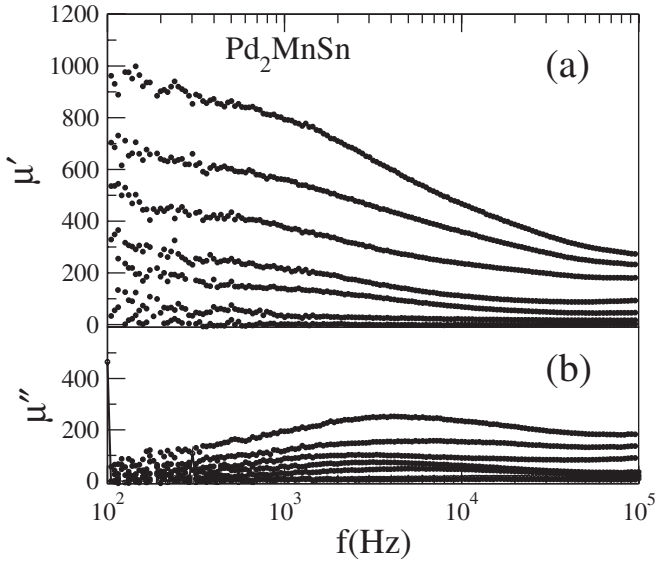

FIG. 5. Frequency dependence of the (a) real and (b) imaginary components of the complex permeability, $\mu=\mu'+i\mu''$, for Pd_2MnSn at several temperatures near T_c. From up to down $T=175$, 175.5, 176, 176.5, 177, 178, and 180 K.

Figures 4(a) and 4(b) show μ' and μ'', respectively, as functions of the temperature for the two investigated compounds at frequencies of 5 kHz and 100 kHz. As for the impedance, both the real and imaginary components of the magnetic permeability show a pronounced and sharp maximum near T_C which is due to the Hopkinson effect. The real part μ' has nearly the same magnitude for both compounds at the Hopkinson peak in $f=100$ kHz. However, at $f=5$ kHz, $\mu'=650$ for Pd_2MnSn and $\mu'=200$ for Pd_2MnSb at the peak. The dissipative component of the magnetic permeability, μ'', is significantly larger for Pd_2MnSn in the whole ferromagnetic range for a fixed frequency.

An analogous procedure as the one above described for determining $\mu(T)$ was employed to obtain the frequency dependence of the complex magnetic permeability. Figures 5(a) and 5(b) display representative results for μ' and μ'' as functions of the frequency in the case of Pd_2MnSn. For all isotherms in the ferromagnetic phase μ' is a decreasing function of the frequency, whereas μ'' shows a broad and weakly temperature dependent maximum in frequencies between 10^3 and 10^4 Hz. The same analysis was made for Pd_2MnSb but in this case the complex permeability is weakly frequency dependent (results not shown).

V. DISCUSSION

A. The Hopkinson effect

The behavior of the initial pemeability in Figs. 4(a) and 4(b) is remarkable. With the rise in temperature, permeability first increases, goes through a sharp maximum at a temperature closely below T_c, then decreases abruptly to the unitary value at T_c. The enhancement of μ is often attributed to a decrease of the magnetocrystalline anisotropy as the temperature approaches T_c, making easier the motion of domain

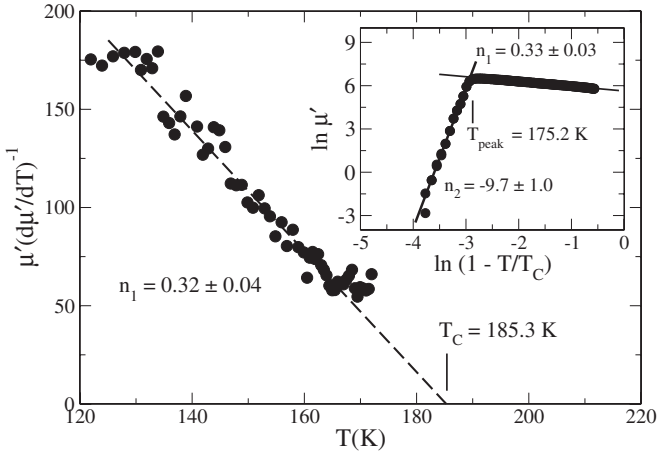

FIG. 6. Kouvel-Fisher plot for the real component μ' measured at 5 kHz for Pd_2MnSn near the Curie temperature. The inset shows a logarithmic plot of μ' versus the reduced temperature.

walls. Depinning of the walls is expected when the anisotropy goes to zero at some temperature below T_c.[24] Reorientation of the magnetization may also be important, mainly in single-domain particles.[14] Since the magnetization decreases strongly when the temperature approaches T_c, a maximum in μ is expected at a temperature T_{peak} nearly below T_c. However, the sharpness of the maxima observed in Figs. 4(a) and 4(b) indicate the possibility that critical fluctuations of the domain walls underlie the Hopkinson effect in the soft ferromagnets Pd_2MnSn and Pd_2MnSb. In uniaxial ferromagnets, a continuous phase transition from Bloch walls to the so-called linear-wall structure at some temperature below T_c was theoretically predicted by Bulaevskii and Ginzburg.[25] These authors also predicted that, although the linear solution may not exist in a cubic crystal, the Bloch walls are not stable close enough to the Curie point, and a transition to another wall structure should occur in this case as well. Evidences of a critical transition between Bloch and linear domain walls were observed in measurements of the kinetic coefficient of the wall relaxation in anisotropic ferromagnets.[26,27]

In Fig. 6 we show a Kouvel-Fisher plot[28] for the real component μ' measured at 5 kHz for Pd_2MnSn. Assuming that the permeability diverges as T approaches the peak temperature from below as a power law given by

$$\mu' = \mu(0)t^{-n_1}, \tag{3}$$

where $t=1-T/T_c$ and $\mu(0)$ is a constant amplitude. The identification of a linear regime in the Kouvel-Fisher (KF) plot allows the simultaneous identification of T_c and the exponent n_1. The critical temperature is given by the intersection of the fitted straight line with the T axis, whereas $1/n_1$ is given by the slope of the fitted line.

From the straight line in Fig. 6, we determine $T_c = 185.3$ K and $n_1 = 0.32 \pm 0.04$. The obtained value for the critical temperature is in reasonable agreement with the Curie temperature for Pd_2MnSn determined from static methods,[29] and is approximately 10 K above T_{peak}. Because of the rounding effects introduced by the numerical derivative in the K-F method, we could not analyze with this method the data in the region above T_{peak} and below T_c, where μ' decreases deeply with temperature. We thus plot $\ln \mu'$ versus $\ln t$, using for T_c the value obtained in the K-F analysis. This graph is displayed in the inset of Fig. 6. These results show that above T_{peak}, μ' may also be described by a power law of t with the exponent $n_2 = -9.7 \pm 1.0$.

Analyses similar to that shown in Fig. 6 were performed for the same sample at 20 kHz and 100 kHz. The obtained parameters are listed in Table I. Parameters obtained for Pd_2MnSb are also shown in Table I. At $f=100$ kHz, the temperature range where the scaling is obeyed is restricted to a short interval below T_{peak} for both samples. The exponent n_2 could not be determined in the high frequency limit.

In low frequencies, the initial permeability is basically governed by domain-wall motion.[9] Based on the phenomenological ansatz, $\mu = 2M_s x/Hd$,[30] where M_s is the saturation magnetization, x is the domain-wall displacement, and d is the domain-wall width, one obtains that the permeability varies as the ratio x/d. In addition, we consider that x scales as $\epsilon_\parallel$, where $\epsilon_\parallel$ is the correlation length for the bulk longitudinal magnetization. On the other hand, the domain-wall width grows as $d \sim (L^2 \epsilon_\perp)^{1/3}$, where L^2 is the domain surface and $\epsilon_\perp$ is the correlation length for the Bloch-wall order parameter.[26] Then, assuming that both correlation lengths diverges at T_c as predicted by the mean-field theory, that is, $\epsilon \sim t^{-1/2}$, we obtain that $\mu \sim t^{-1/3}$. Though crude, the above model describes approximately the behavior of μ' below

TABLE I. Values of the Curie temperature, peak temperature, and critical exponents for Pd_2MnSn and Pd_2MnSb obtained from Kouvel-Fisher analyses and $\ln \mu'$ vs $\ln t$ plots at severals frequencies.

		Kouvel-Fisher plot		$\ln \mu'$ vs $\ln t$ plot		
	f(Hz)	T_c (K)	$n_{1(K-F)}$	n_1	$-n_2$	T_{peak} (K)
Pd_2MnSn	5 kHz	185.3	0.32±0.03	0.33±0.03	9.7±1.0	175.2
	20 kHz	184.4	0.32±0.03	0.30±0.04	6.4±0.8	174.8
	100 kHz	182.3	0.24±0.03	0.24±0.04		
Pd_2MnSb	5 kHz	244.2	0.25±0.03	0.31±0.03	7.0±0.8	238.3
	20 kHz	243.8	0.20±0.01	0.24±0.03	5.1±0.6	238.3
	50 kHz	243.5	0.20±0.02	0.25±0.03	7.4±0.9	238.1
	100 kHz	242.3	0.20±0.02	0.18±0.02		

T_{peak} at low frequencies. Along the same lines, one may also understand why the scaling regime for the permeability shrinks towards the high-temperature range when $f = 100$ kHz. Indeed, in high frequencies the domain-wall displacements might not follow the field oscillations. Then, at low temperatures and strong enough pinning, permeability should depend on strong relaxational effects.

Above T_{peak}, permeability decreases steeply and also scales with T_c. However, the large values encountered for the n_2 exponent suggests that dynamic effects are important in this temperature range. A possible scenario is that μ is dominated by a critical slowing down above T_{peak}. The abrupt change of behavior may be related to the theoretically predicted instability of Bloch walls at a temperature below T_c.[25] Depinning and reduction of the magnetocrystalline anisotropy may also underlie the crossover at T_{peak}. Assuming a Debye-type dynamics,[31] one would expect that $\mu' \sim \bar{\tau}^{-2}$, where $\bar{\tau}$ represents the mean relaxation time associated with domain-wall motion [see Eq. (4)]. The theory of dynamical critical scaling predicts that[32] $\bar{\tau} \sim \xi^z$, where ξ is the correlation length of the domain-wall order parameter,[26] and z is the dynamical exponent. One then obtain $\mu' \sim t^{-2z\nu}$, where ν is the static exponent for the correlation length. If disorder is relevant,[33] both z and ξ may be large enough to justify the experimentally observed n_2.

In an alternative scenario, the steep decrease of μ' above T_{peak} may result from a nonequilibrium process as jumps and avalanches. In this case, the observed power-law scaling with the reduced temperature would merely represent an effective behavior related to the critical reduction of the magnetization that tends to zero at T_c.

We do not study in detail the permeability in the close vicinity of T_c. In the paramagnetic range, μ should mimic the critical divergence of the susceptibility. Immediately below T_c, the critical behavior of the magnetization should be relevant to describe the temperature dependence of both the real and imaginary components of μ.

B. Dynamical effects

Figure 5(a) shows that the real part of the low-frequency permeability in Pd_2MnSn reaches a much higher value than that in Pd_2MnSb. The same occurs with the imaginary component. In the high-frequency limit, μ' has comparable magnitudes for both compounds, whereas μ'' is still much higher in Pd_2MnSn than in Pd_2MnSb. We suggest that the high values observed for μ' in Pd_2MnSn at low frequencies are related to the characteristic APB's in this compound. Mechanical stresses produced by thermal contraction during the sample solidification after fusion produce extended APB fields in Pd_2MnSn. This effect is also observed in quenched Cu-Mn-Al Heusler alloys.[34] We believe that many of these APB's are not eliminated by the subsequent thermal annealing in Pd_2MnSn. The presence of APB's favors the formation of domain walls. In the opposite sides of these interfaces, the Mn spins couple antiferromagnetically so that an APB is itself a 180° domain wall. Although these walls are expected to be efficiently pinned, those connected to the edges of the APB's may significantly bulge under the action of the self-field. Thus, the occurrence of a large number of APB's in Pd_2MnSn is probably the property underlying the relatively high value of the low-frequency permeability of this compound when compared to that of Pd_2MnSb.

In the studied range of frequencies, the magnetic permeability in soft magnets is mainly due to domain-wall oscillations. However, as f increases the domain walls become unable to follow the self-field oscillations, and damping effects become relevant. When the dispersion is relaxational, the complex permeability can be described phenomenologically by the modified Debye formula,[35]

$$\mu = \mu_S + \frac{\mu_T - \mu_S}{1 + (i\omega\bar{\tau})^{1-\alpha}}, \tag{4}$$

where μ_T is the isothermal permeability in the low-frequency limit ($\omega\bar{\tau} \ll 1$), μ_S is the adiabatic permeability in the high-frequency limit ($\omega\bar{\tau} \gg 1$), and α ($0 \leqslant \alpha < 1$) determines the width of the relaxation time distribution around $\bar{\tau}$. For $\alpha = 0$ one has the original Debye formula with a single relaxation time.[31] The limit $\alpha = 1$ accounts for a distribution of infinite width. The behavior described by Eq. (4) has been observed in the complex susceptibility of spin glasses[36] and uniaxial ferromagnets.[37]

Equation (4) may be separated into real and imaginary parts, so that the relation below is obtained

$$\mu'' = -\frac{\mu_T - \mu_S}{2\tan[(1-\alpha)\pi/2]} + \sqrt{(\mu_T - \mu')(\mu' - \mu_S) + \frac{(\mu_T - \mu_S)^2}{4\tan^2[(1-\alpha)\pi/2]}}. \tag{5}$$

For $\alpha = 0$ this equation represents an arc of a semicircle in the Argand diagram (or Cole-Cole plot[35]) with its center lying on the real axis.[38]

To investigate the dispersion observed in the complex permeability of Pd_2MnSn, we plot μ'' as a function of μ' in Fig. 7 for several temperatures near T_c. The solid lines are fits to Eq. (5) that indeed provides an adequate description of the experimental data. The distribution parameter amounts to $\alpha \simeq 0.32$ and does not change noticeably when the temperature increases toward T_c. This value for α indicates that a broad distribution of relaxation times occurs in association with different sizes of magnetic domains. Moreover, the nearly constant value for α shows that the overall domain structure does not change significantly when the temperature approaches T_c, in spite of the large temperature dependence of the isothermal magnetic permeability μ_T.

VI. CONCLUSIONS

In summary, we have measured the complex impedance of the compounds Pd_2MnSn and Pd_2MnSb as a function of temperature and frequency of the alternating current. By computational analysis of the experimental data, the magnitude, as well as the temperature and frequency dependence of the complex initial permeability, were obtained.

Both samples show a sharp maximum on the real and imaginary components of the magnetic permeability in a

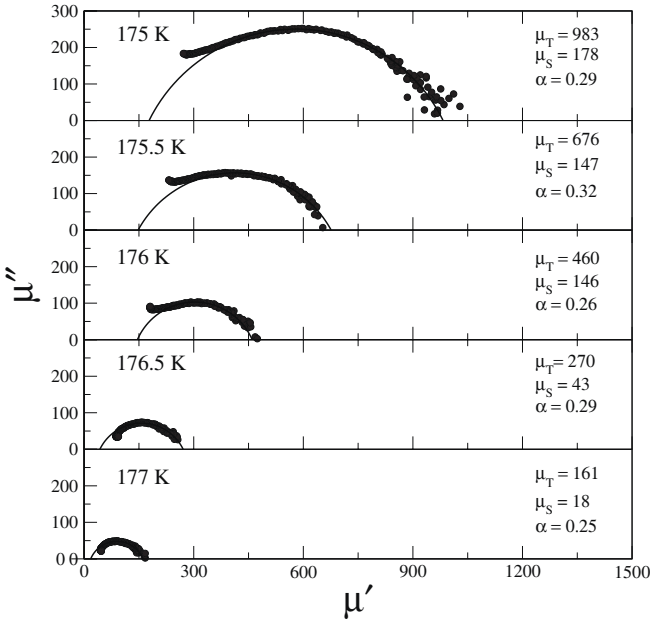

FIG. 7. Argand diagrams of $\mu(f)$ for Pd_2MnSn at different temperatures near T_c. Frequency varies from right (100 Hz) to left (100 kHz). Full lines are fits to the modified Debye formula, Eq. (5).

characteristic temperature, T_{peak}, located closely below T_c. This behavior is known as the Hopkinson effect. We analyze the temperature dependence of the real part of the permeability above and below T_{peak} in both compounds and show that μ' behaves as the power law of the reduced temperature $1-T/T_C$ in this temperature region. We suggest that a cross-over involving the domain-wall fluctuations occurs at T_{peak}, since the power law describing the temperature variation of μ' scales with T/T_c both below and above T_{peak}. The critical exponent obtained when T approaches T_{peak} from below is consistent with simple expectations based on mean-field effects of Bloch-wall oscillations in the permeability. Closely above T_{peak} dynamical effects are probably responsible for the steep decrease of both the real and imaginary parts of the permeability.

In low frequencies, the Hopkinson peak is significantly more pronounced in Pd_2MnSn than in Pd_2MnSb. We suggest that this characteristic is related to the existence of a relatively higher density of domain walls in the former compound. These domain walls are generated by antiphase boundaries that easily form in Pd_2MnSn and underlies the soft magnetic properties of this system.

Strong frequency dependence of the magnetic permeability was observed in the ferromagnetic state of Pd_2MnSn. From a Cole-Cole analysis we were able to determine the frequency distribution for different temperatures near T_c. The experimental results were fitted by a modified Debye formula with $\alpha \sim 0.3$. This value for α suggests the occurrence of a wide distribution of relaxation times associated with the motion of domain walls.

As a final conclusion, we emphasize the importance of impedance experiments as a useful technique to study the detailed behavior of soft ferromagnetic materials near the Curie temperature.

ACKNOWLEDGMENTS

This work was partially financed by the Brazilian Ministry of Science and Technology under Grant PRONEX/CNPq No. 66.2187/1996-2.

*Electronic address: fraga@if.ufrgs.br

[1] F. L. A. Machado, C. S. Martins, and S. M. Rezende, Phys. Rev. B **51**, 3926 (1995).
[2] G. L. F. Fraga, P. Pureur, and D. E. Brandão, Solid State Commun. **124**, 7 (2002).
[3] C. Gómez-Polo, J. I. Pérez-Landazabal, V. Recarte, M. Vázquez, and A. Hernando, Phys. Rev. B **70**, 094412 (2004).
[4] V. V. Khovailo and T. Abe, J. Appl. Phys. **94**, 2491 (2003).
[5] M. Carara, A. Gündel, M. N. Baibich, and R. L. Sommer, J. Appl. Phys. **84**, 3792 (1998).
[6] J. Hopkinson, Philos. Trans. R. Soc. London, Ser. A **180**, 443 (1889).
[7] H.-W. Kwon, J. Magn. Magn. Mater. **239**, 447 (2002).
[8] D. Stoppels, J. Appl. Phys. **51**, 2789 (1980).
[9] B. Hoekstra, E. M. Gyorgy, P. K. Gallagher, J. D. W. Johnson, G. Zydzik, and L. G. V. Uitert, J. Appl. Phys. **49**, 4902 (1978).
[10] J. Loaëc, J. Phys. D **26**, 963 (1993).
[11] M. S. Leu and T. S. Chin, J. Appl. Phys. **81**, 4051 (1997).
[12] B. Dieny, B. Barbara, G. Fillon, M. Maeder, and B. Michelutti, J. Phys. (Paris) **48**, 1741 (1987).
[13] J. Geshev, O. Popov, V. Masheva, and M. Mikhov, J. Magn. Magn. Mater. **92**, 185 (1990).
[14] O. Popov and M. Mikhov, J. Magn. Magn. Mater. **75**, 135 (1988).
[15] J. Kötzler and M. Hartl, J. Appl. Phys. **73**, 6263 (1993).
[16] F. Heusler, W. Stark, and R. Haupt, Verh. Dtsch. Phys. Ges. **5**, 200 (1903).
[17] P. J. Webster and R. S. Tebble, Philos. Mag. **16**, 347 (1967).
[18] T. Shinohara, K. Sasaki, H. Yanauchi, H. Watanabe, H. Sekizawa, and T. Okada, J. Phys. Soc. Jpn. **50**, 2904 (1981).
[19] K. Ikeda and S. Takahashi, Phys. Rev. B **30**, 3808 (1984).
[20] T. Kamiyama, T. Shinohara, S. Tomiyoshi, Y. Minonishi, H. Yamamoto, H. Asano, and N. Watanabe, J. Appl. Phys. **68**, 4741 (1990).
[21] L. D. Landau and E. M. Lifshitz, *Electrodynamics of the Continuous Media* (Pergamon Press, Oxford, 1960).
[22] W. H. Schreiner, P. Pureur, and D. E. Brandão, Phys. Status Solidi A **60**, K123 (1980).
[23] D. Meeker, *Finite Elements Method Magnetics, Version 3.1* (2001), http://femm.foster-miller.net
[24] B. D. Cullity, *Introduction to Magnetic Materials* (Addison-Wesley, Reading, 1972).
[25] L. N. Bulaevski and V. L. Ginzburg, Sov. Phys. JETP **18**, 530 (1964).
[26] J. Kötzler, D. A. Garanin, M. Hartl, and L. Jahn, Phys. Rev. Lett. **71**, 177 (1993).
[27] M. Hartl-Malang, J. Kötzler, and D. A. Garanin, Phys. Rev. B **51**,

8974 (1995).
[28] J. S. Kouvel and M. E. Fisher, Phys. Rev. **136**, A1626 (1964).
[29] P. Pureur, G. L. Fraga, J. V. Kunzler, W. H. Schneider, and D. E. Brandão, J. Phys. A **49**, 179 (1988).
[30] G. P. Vella-Coleiro, D. H. Smith, and L. G. V. Uitert, J. Appl. Phys. **43**, 2428 (1972).
[31] P. Debye, *Polar Molecules* (Chemical Catalogue Company, New York, 1929).
[32] P. C. Hohenberg and B. I. Halperin, Rev. Mod. Phys. **49**, 435 (1977).
[33] I. A. Campbell, Phys. Rev. B **37**, 9800 (1988).
[34] A. J. Lapworth and J. P. Jakubovics, Philos. Mag. **29**, 253 (1974).
[35] K. S. Cole and R. H. Cole, J. Chem. Phys. **9**, 341 (1941).
[36] C. Dekker, A. F. M. Arts, and H. W. de Wijn, Phys. Rev. B **40**, 11243 (1989).
[37] M. Grahl and J. Kötzler, J. Phys.: Condens. Matter **75**, 527 (1989).
[38] D. Hüser, A. J. van Duyneveldt, G. J. Nieuwemhuys, and J. A. Mydosh, J. Phys. C **19**, 3697 (1986).